

Geometric robust descriptor for 3D point cloud

Seung Hwan Jung, Yeong-Gil Shin, and Minyoung Chung*

Abstract—We propose rotation robust and density robust local geometric descriptor. Local geometric feature of point cloud is used in many applications, for example, to find correspondences in 3D registration and to segment local regions. Usually, application accuracy depends on the discriminative power of the local geometric features. However, there are some problems such as point sparsity, rotated point cloud, and so on. In this paper, we present new local feature generation method to make a rotation robust and density robust descriptor. First, we place kernels aligned around each point and align them to the normal of the point. To avoid the sign problem of the normal vector, we use symmetric kernel point distribution with respect to the tangent plane. Next, from each kernel point, we estimate geometric information which is rotation robust and discriminative. Finally, we operate convolution process with consideration of kernel point structure, and aggregate all kernel features. We experiment our local descriptors on the ModelNet40 dataset [1] for registration and classification, and the ShapeNet part dataset [2] for segmentation. Our descriptor shows discriminative power regardless of point distribution.

Index Terms—Rotation robust descriptor, 3D point cloud, registration, classification, part segmentation.

I. INTRODUCTION

POINT clouds have been widely used in many application fields, including robotics, autonomous driving, and augmented/mixed reality as 3D sensor can capture rich geometric information. Estimation of an optimal transformation in registration based on correspondence between two objects. To deal with point clouds in 3D registration, extracting salient local geometric information is a key task. Early work on local geometric feature was based on hand-crafting based methods. While end-to-end learning are becoming feasible for 3D point cloud analysis, due to recent advances in deep learning field, the robust local feature descriptor generation remains a challenge in the field of computer vision research.

Descriptors for point cloud applications have been a wide research area for point cloud registration, model segmentation, and classification. PointNet [3] shows the new paradigm for point cloud analysis with permutation invariant method, but cannot encode the local geometric information. To encode the local geometric information, PPFNet [4] uses PointNet for local regions and DGCNN [5] encodes relative position of neighbors for each point. In practical, point cloud data captured by sensors are usually not aligned to the same frame and irregularly distributed. However, these method do not build rotation invariant descriptors, and these method are affected by point cloud density. KPConv [6] uses kernel points around each point cloud for efficiently handle irregularly distributed

point clouds. KPConv shows satisfactory performance, but do not consider rotational information. 3DSmoothNet [7] extracts local region points and aligns the local points to the local reference frame of the center point. However, a sign of a normal axis and directions of the other two axes is not unique in planar region. Lastly, one common problem with a descriptor is that local descriptors from monotonous and repeating area may be non-salient descriptors, and these descriptors are not useless in 3D registration.

To overcome the previous limitation, we propose a rotation robust and point distribution robust descriptor generation method. Our method is inspired by KPConv [6] and 3DSmoothNet [7]. KPConv deals with point clouds similar to 2D image-based convolution using kernels located around points, and the method is efficient and robust to irregular structured point clouds. 3DSmoothNet generates voxel-based descriptor from aligned local points using local reference frame. Inspired by these idea, we align the kernels to the normal vector, and extract rotation invariant features. Due to the non uniqueness property of local reference frame in the planar region, we distribute kernels in a form of cylinder shape. This shape is symmetric about a tangent plane to handle the sign problem, and has the circular cross section to handle the other inaccurate reference axes. With this kernel structure, we apply convolution with adjacent kernels together in a way that is not affected by rotation to increase representative power. In addition, to increase representative power of a descriptor from monotonous and repeating area, we aggregate all features based on distances from each point to build discriminative global features.

The major contributions of this work can be summarized as follows:

- The proposed descriptor encodes rotation-robust feature
- The proposed convolution method with the symmetric kernel structure effectively gather structural information invariant to the sign problem
- We experiment our method on several benchmark datasets

To demonstrate our feature descriptor, we experiment our method on three kinds of tasks: classification, registration and segmentation. We train and test on ModelNet40 [1] for classification and registration, and ShapeNet [2] for segmentation. We show discriminative power of our descriptor.

II. RELATED WORKS

A. Hand-crafted 3D features

Before advance of deep learning, 3D feature descriptor was hand-crafting descriptors. Local descriptors are generated based on the relationship between a point and spatial neighborhoods around the point. In addition, some methods build rotation invariant descriptor based on a local reference frame.

Asterisk indicates corresponding author.

S. H. Jung, Y.-G. Shin, and *M. Chung are with the Department of Computer Science and Engineering, Seoul National University, Korea (e-mail: chungmy@snu.ac.kr).

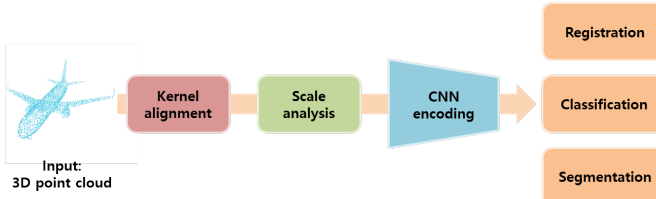


Fig. 1: Overview.

Spin Images [8] aligns neighbors using the surface normal of the interest point and represents aligned neighbors to cylindrical support region using radial and elevation coordinates. 3D Shape Context [9] represents neighbors in the support region with grid bins divided along the azimuth, elevation, and radial values. USC [10] extends the 3D Shape Context method by applying the local reference frame based on the covariance matrix of points. Similarly, SHOT [11] also calculates the local reference frame and builds a histogram using angles between point normals. PFH [12] and FPFH [13] estimate pairwise geometric differences. Application area of these methods are usually limited to the registration area if there is no additional machine learning methods, but ideas of these methods give inspiration to many deep learning based descriptor methods.

B. Deep learning based 3D features

1) *Volumetric based Methods*: These methods attempt to approximate the point cloud data into regular volumetric representation, and process the approximated data similar to 2D image-based methods [14] [15].

Since the number of dimensions is limited by hardware performance, these methods approximate the data into low resolution volumetric representation. To overcome this problem, some methods represent point cloud data with efficient way. OctNet [16] divides the space using a set of unbalanced octrees based on the sparsity. Some methods [17] [18] [19] use sparse tensor which only saves the non-empty space coordinates and features. These methods not only reduce memory usage but also reduce run-time significantly.

To build rotation invariant descriptor, 3DSmoothNet [7] calculates the local reference frame based on the covariance of points and transforms neighbor points within the spherical support area of the interest point using the local reference frame before voxelizing the points. However, a sign of a normal axis and directions of the other two axes is not unique in planar region. To deal with this situation, we assume the sign of the normal vector is not unique. In addition, to deal with the inaccurate remaining reference axes, kernels distributed in circular shape on the tangent plane is suitable rather than kernels distributed in square shape like a volumetric representation. Therefore, we use customized kernel similar to the KPConv [6] method which distributes kernels around each point.

2) *Point based Methods*: PointNet [3] and PointNet++ [20] are the pioneer point cloud deep learning methods. The methods encode unstructured point cloud using a shared multi-layer perceptron, and build the permutation invariant descriptor

using a global max-pooling. Based on PointNet, some methods have been developed. PPFNet [4] extends PointNet [3] to learn local geometric features. PPFNet builds local features using PointNet, and then fuses global information extracted from the local features using a max-pooling to produce discriminative local descriptors. PPF-FoldNet [21] learns descriptor using folding-based auto encoding for unsupervised learning, and uses rotation invariant features. DGCNN [5] selects k-nearest neighbors for each point and encodes descriptors using relative neighbor locations from a point to encapsulate the geometric information. KPConv [6] proposes Kernel Point Convolution method which places kernel points around each point to efficiently handle irregularly distributed point clouds and aggregates the geometric information from the kernel points. We extend the KPConv method by applying normal vectors. As described in the KPConv, the normal vector is available for artificial data. Because the sign of normal vector can be changed. Therefore, we use unsigned normal vectors for aligning kernels and estimating features.

III. METHOD

Figure 1 shows an overview of our descriptor generation framework. We represent each point using information getting from kernels around the point inspired by KPConv [6]. To build rotation robust kernels, we use normal vectors of each point to align the kernels (Section 3.1). We then extract local information from kernels and aggregate to build descriptor (Section 3.2) and estimate global information (Section 3.3). Next, we apply convolution with the kernels invariant to the sign problem (Section 3.4). Lastly, to build scale robust descriptor, we apply scale adaptation module to the network (Section 3.5).

A. Aligned kernel

Kernels are used to gather geometric information around each point from each kernel's point of view. To do this, kernels have to be distributed uniformly around each point not only to analyze geometric information from various point of view but also to extract similar point of view as much as possible if there is no orientation information.

Usually orientation information is estimated based on the covariance of points, and the other reference axes are estimated by projecting the vector from the interest point to the weighted averaged neighbors to the plane orthogonal to the normal. These are not unique if the point is located on planar surface, but among the three local reference vectors, the normal direction is reliable. Therefore, we focus on the tangent plane direction rather than normal direction to maximize overlapped receptive field of kernels. We place kernels in the form of a cylinder shape around each point, and align the cylinder to the reference axes.

Figure 2(a) shows our kernel distribution. Cross section of the cylinder is the circle along the normal direction. We place from 5 to 6 kernels for each circle, and group them as one layer. Lastly, the cylinder consists of 2 to 3 layers.

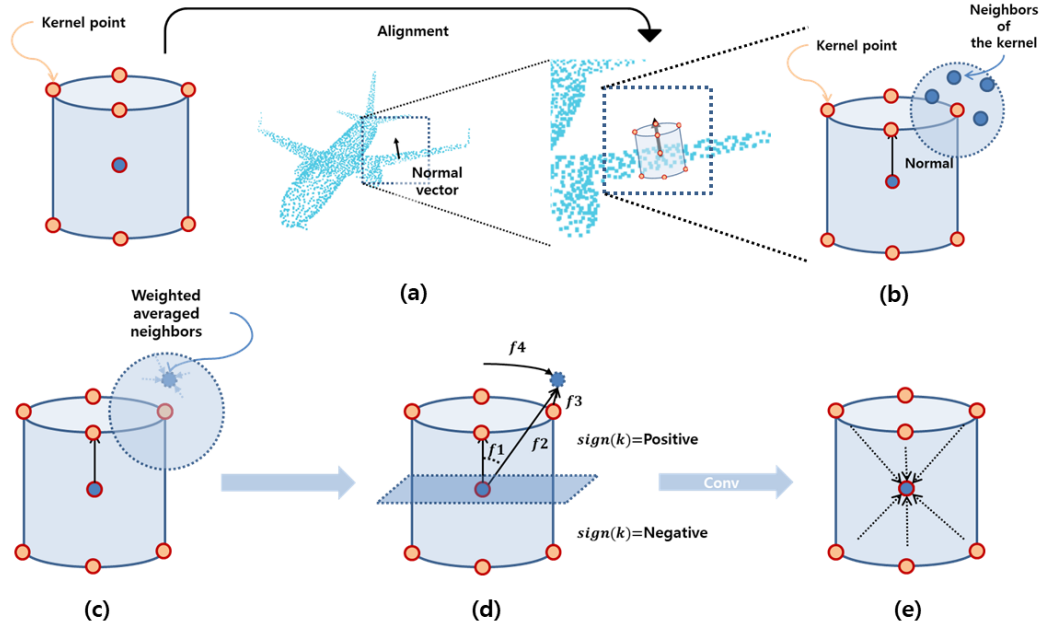


Fig. 2: (a) Kernel points are aligned using the normal vector of target point. (b) Neighbors are selected for each kernel point. (c) Weighted averaged location is estimated based on the distance from the kernel point to the neighbors. (d) Four features are estimated for each kernel point. (e) After convolution, each kernel features are aggregated.

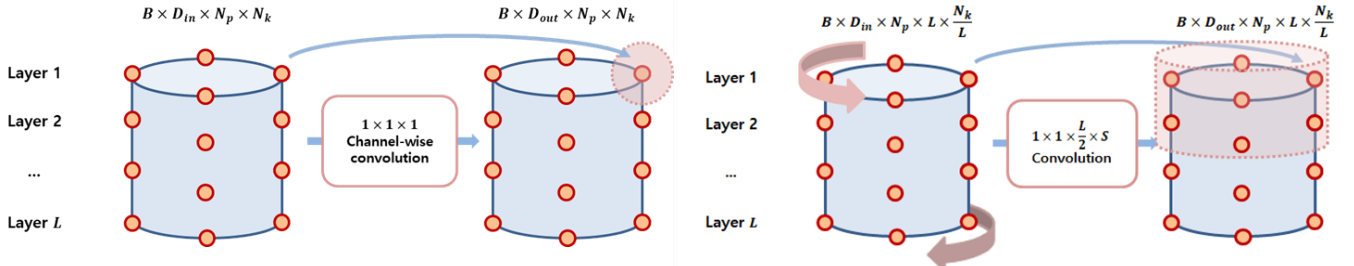


Fig. 3: Left: Channel-wise convolution, Right: Circular convolution. The red transparent region indicates the receptive field. S indicates the convolution kernel size.

B. Rotation invariant geometric information

Next step is to estimate rotation invariant features for each aligned kernel.

First, we extract k -nearest neighbor points from each kernel, and calculate weighted averaged location based on their distance from the kernel (Eq. 1). As a weight term, we use gaussian function to reduce the influence of outliers.

$$\hat{x}_i^k = \sum_{x_j \in N(x_i^k)} \frac{w_j x_j}{\sum w_j} \text{ where } w_j = \exp\left(-\frac{(x_j - x_i^k)^2}{d^2}\right) \quad (1)$$

$\hat{x}_i^k \in \mathbb{R}^{N \times 3}$ is the weighted averaged location of the k -th kernel point of x_i , and d indicates the distance from the center point to the kernel point.

To build rotation robust and discriminative descriptor, we estimate four kinds of features. we first estimate angles between two vectors, one is from the center point of kernels to the weighted averaged point, and the other one is normal vector.

However, since the normal vector has the normal orientation problem, we multiply negative sign to the normal vector if the kernel is located at below the tangent plane (Eq. 2). v_i indicates the normal vector of x_i . $\text{sign}(k)$ returns negative sign if the kernel is located at below the tangent plane. This term helps to estimate the angle value regardless of the normal sign. Next, we estimate distances from the interest point to the averaged neighbors and from the kernels to the averaged neighbors. To provide direction to the closest adjacent kernel points, we estimate distance ratio from two adjacent kernel points to the averaged point (Eq. 5). Using these features, kernel point can specify relative location of the averaged neighbor points from the kernel. In addition, these features are rotation invariant features. Figure 2(d) shows the geometric information extraction process.

$$f1_i^k = v_i \cdot \frac{\hat{x}_i^k - x_i}{\|\hat{x}_i^k - x_i\|} \cdot \text{sign}(k) \quad (2)$$

$$f2_i^k = \left\| \frac{\hat{x}_i^k - x_i}{d} \right\| \quad (3)$$

$$f3_i^k = \left\| \frac{\hat{x}_i^k - x_i^k}{d} \right\| \quad (4)$$

$$f4_i^k = \frac{\left\| \hat{x}_i^k - x_i^{k+1} \right\|}{\left\| \hat{x}_i^k - x_i^{k+1} \right\| + \left\| \hat{x}_i^k - x_i^{k-1} \right\|} \quad (5)$$

C. global information

Above features describe local region of the point cloud. To increase representative power of a descriptor from monotonous and repeating area, we estimate global information from local information. Rather than building single global feature for all points, we estimate adaptive global features for each point. For each point, we calculate weights for the other points based on the gaussian distances between points, and then calculate weighted average based on the weights.

D. Circular convolution

With these features, we then process the convolution step. Since we align the kernels using only normal axis, each kernel is not aligned to unique local reference frame, and the order of kernels may be changed depending on the point distribution. However, within the cylinder layer, adjacent kernels are not changed. Therefore, we extend 1x1x1 channel-wise convolution Eq. 6 to Eq. 7.

$$x_i = \sum_{\hat{x}_i^k} f(g(\hat{x}_i^k)) \quad (6)$$

$$x_i = \sum_{\hat{x}_i^k} f(g(\hat{x}_i^{c(k,-1)})) \square g(\hat{x}_i^k) \square g(\hat{x}_i^{c(k,+1)}) \quad (7)$$

$c(k, +1)$ means the clockwise adjacent kernel point of the k -th kernel point in the cylinder layer, and $c(k, -1)$ means the counterclockwise adjacent kernel point. However, this convolution process is also affected by order of adjacent kernels due to the sign problem of normal vectors. To avoid this problem, we divide the kernel points into two groups, one is collection of kernels above the tangent plane, and the other one is collection of kernels below the tangent plane. We select adjacent kernel in clockwise order if the kernel belongs to the first group, i.e. the kernel is located at positive normal direction. Otherwise, we select in counterclockwise order if the layer is located at negative normal direction. In addition, we process convolution with multiple layers if the layers belong to the same group. Eq. 7 is extended to the Eq. 8. $adj(k)$ indicates a set of adjacent kernel points of the k -th kernel point in the same group. To do this, we use circular padding convolution operation.

$$x_i = \sum_{\hat{x}_i^k} f(g(\hat{x}_i^k)) \square_{j \in adj(k)} g(\hat{x}_i^j) \quad (8)$$

Figure 3 shows the convolution process using kernels. After convolution, kernel features around target point are aggregated by summation or maximum value selection to build the point feature.

E. Scale adaptation module

Our features mentioned above are invariant to rotation, but depend on a distance from an interest point to the kernel of the point, and the kernel size is related to the scale of the point cloud. If the kernel size determined by a heuristic way is too small or too large, it cannot properly encode the geometric information. To build descriptor robust to the scale, we propose a method to adapt the kernel size based on the model geometric. First, we roughly select two kernel sizes and build features using the kernel sizes. Features are fed to the module, and the interpolation weight is estimated as the output of the module through convolution operations. Next, we use interpolated two kernel sizes using the interpolation weight and build descriptor with the interpolated kernel size.

IV. RESULT

A. Registration

We experiment our method on the ModelNet40 registration [1] to demonstrate the rotation robustness. ModelNet40 contains 12,311 meshed CAD models from 40 categories. ModelNet40 is split by category into training and test sets, and the first 20 categories among the 40 categories are used for training. For each model, we use 1,024 points for training and testing.

DCP [22] shows the end-to-end network for rigid registration. Inspired by the method, we use the SVD module to compute a rigid transformation after building features. Figure 4 (a) shows registration architecture. As evaluation metrics, mean squared error (MSE), root mean squared error (RMSE), and mean absolute error (MAE) are used for rotation and translation.

Table I shows the registration results on the remaining categories. Our method outperforms in both rotation and translation estimations compared to the other methods. Even when compared to the results trained using all categories, our method shows significantly better performance. Figure 5 shows the comparison of the registration results. Results of DCP show small differences between two point clouds, but results of ours show almost overlapped point clouds. These results mean that mapping between the source and target points based on the encoded features are accurate, and there is almost no duplicated or wrong correspondence. It shows that our encoded features have discriminative power.

B. Classification

Next, we experiment our method on the ModelNet40 for classification [1]. Among 12,311 models, 9,843 models are used for training and remaining 2,468 models are used for testing. For each model, we use 1,024 points for training and testing.

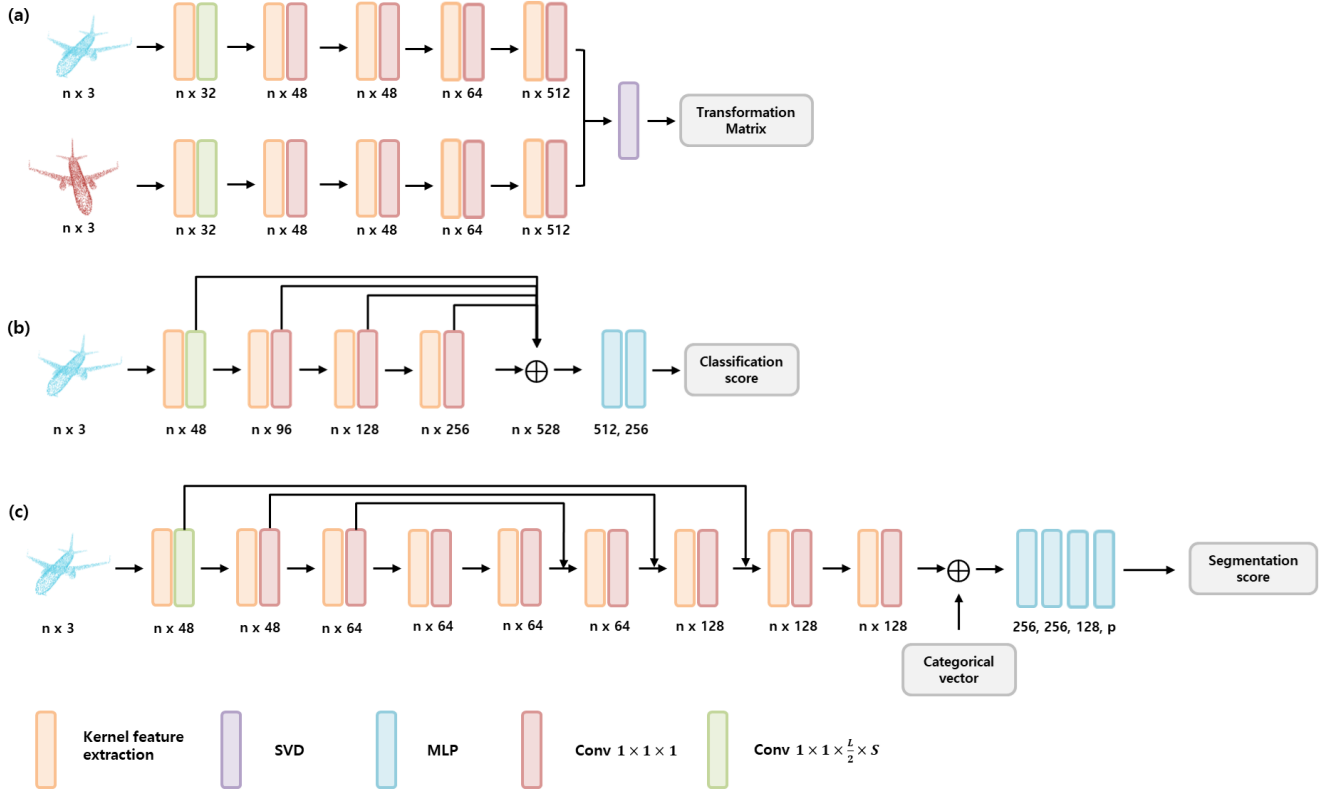


Fig. 4: (a) Network architecture for registration. (b) Network architecture for classification. (c) Network architecture for part segmentation

Method	R-MSE	R-RMSE	R-MAE	T-MSE	T-RMSE	T-MAE	C
ICP	892.601135	29.876431	23.626110	0.086005	0.293266	0.251916	-
Go-ICP [23]	192.258636	13.865736	2.914169	0.000491	0.022154	0.006219	-
FGR [24]	97.002747	9.848997	1.445460	0.000182	0.013503	0.002231	-
PointNetLK [25]	306.323975	17.502113	5.280545	0.000784	0.028007	0.007203	20
PointNetLK [25]	227.870331	15.095374	4.225304	0.000487	0.022065	0.005404	40
DCP-v2 [22]	9.923701	3.150190	2.007210	0.000025	0.005039	0.003703	20
DCP-v2 [22]	1.307329	1.143385	0.770573	0.000003	0.001786	0.001195	40
Our method	0.017159	0.130991	0.064475	0.000000	0.000048	0.000027	20

TABLE I: ModelNet40 registration results. Evaluation metrics are mean squared error (MSE), root mean squared error (RMSE), and mean absolute error (MAE) for rotation (R) and translation (T). C indicates the number of categories for training.

We use DGCNN [5] classification architecture as our baseline. First, four convolution layers are used to extract geometric information, then concatenate four results to provide multi-scale features. In addition, to increase representation power, we estimate global context using local features and apply attention module. Finally, global feature is extracted and fully-connected layers are used to predict the model class. Table II shows the classification results. Although our method is focused on the rotation robust descriptor, our descriptor achieves the comparable performance with the state-of-arts.

C. Segmentation

We experiment our method on the ShapenetPart for part segmentation [2]. ShapenetPart contains 16,681 3D models from 16 categories. Each point is annotated with part labels.

ShapenetPart consists of 50 kinds of parts, and models consist of from 2 to 6 parts. For each model, we use 2,048 points for training and testing.

In the segmentation experiment, we use U-Net without additional down and up-sampling layers as our segmentation architecture. To evaluate the result, we use Intersection-over-Union (IoU). Similar to the KPConv [6], we add the positions as additional features. Table III shows the segmentation results.

D. Parameter and ablation study

We experiment our methods with some parameter settings on the ModelNet40 registration. We change convolution operation, the number of kernels, the number of nearest neighbors for each kernels, and usage of the additional module.

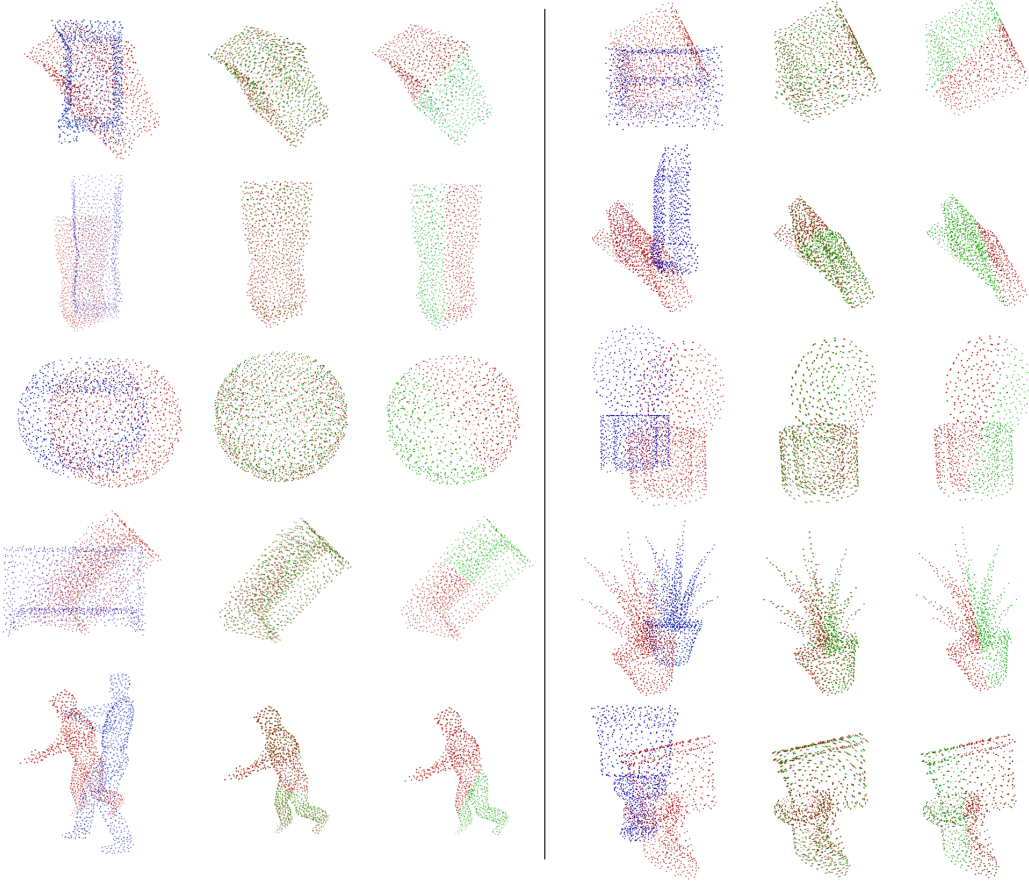


Fig. 5: Left: source (blue) and target (red) point clouds, Middle: registration results of DCP [22]. Green indicates the transformed source point clouds. Right: registration results of our method.

Method	Mean Class Accuracy	Overall Accuracy
3DShapeNets [1]	77.3	84.7
VoxNet [14]	83.0	85.9
Subvolume [15]	86.0	89.2
VRN (single view) [26]	88.98	-
VRN (multiple views) [26]	91.33	-
ECC [27]	83.2	87.4
PointNet [3]	86.0	89.2
PointNet++ [20]	-	90.7
Kd-net [28]	-	90.6
PointCNN [29]	88.1	92.2
PCNN [30]	-	92.3
DGCNN [5]	90.2	92.9
Our method	88.9	91.8

TABLE II: ModelNet40 classification results

First, we experiment the convolution methods from the $1 \times 1 \times 1$ channel-wise convolution to the circular convolution method. The results show significantly better performance in both rotation and translation. With the circular convolution method. These results mean that convolution operations with structure information can analyze the kernel features properly.

Second, we experiment the effect of the number of kernels. Network with a larger number of kernels shows increased performance. As the number of kernels increases, the range covered by the descriptor also increases, resulting in better performance.

Third, to check the effect of the number of neighboring points on the stability, we experiment the network with a smaller number of neighbors. Although we reduce the number of neighbors for each kernel point, performance of the network using a smaller neighbors is comparable with that of the network using a larger neighbors. Since neighbors are selected from each spatially well-distributed kernel, the number of neighbors does not significantly affect to the results.

Fourth, we estimate global features using the local features of the last layer and concatenate the features to the local features. As a result, rotational error is decreased. This means that

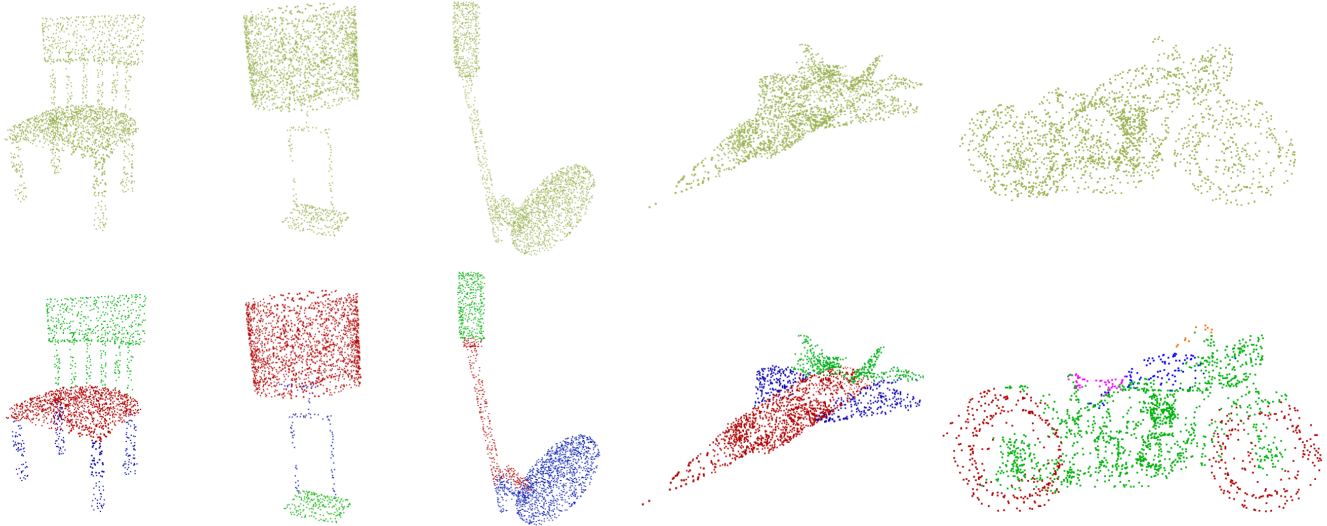


Fig. 6: Top: source points. Bottom: part segmentation results

Method	mIoU
SPLATNet [31]	85.4
SGPN [32]	85.8
3DmFV-Net [33]	84.3
SynSpecCNN [34]	84.7
RSNet [35]	84.9
SpecGCN [36]	85.4
PointNet++ [20]	85.1
SO-Net [37]	84.9
PCNN by Ext [30]	85.1
SpiderCNN [38]	85.3
MCCConv [39]	85.9
FlexConv [40]	85.0
PointCNN [29]	86.1
DGCNN [5]	84.7
SubSparseCNN [33]	86.0
KPCConv [6]	86.2
Our method	83.8

TABLE III: ShapeNetPart segmentation results

the global features help to disambiguate each local descriptor.

V. CONCLUSION

In this paper, we propose a generation method for 3D point cloud. Kernel points distributed in a cylinder shape are aligned to a normal vector of a point. Each kernel points takes neighbor points and extract rotation robust geometric information. We then apply circular padding convolution operation to refer nearby kernel information to increase representation power. Finally, we experiment our method on the registration, classification and segmentation tasks. Our method shows satisfactory performance. Especially, it shows out-performance in registration using rotation robust features and structural convolution. In practical, 3D point cloud data captured by sensors may be not aligned. We expect our method help to analyze 3D data in more general situation.

REFERENCES

- [1] Zhirong Wu, S. Song, A. Khosla, Fisher Yu, Linguang Zhang, Xiaou Tang, and J. Xiao, “3d shapenets: A deep representation for volumetric shapes,” in *2015 IEEE Conference on Computer Vision and Pattern Recognition (CVPR)*, 2015, pp. 1912–1920.
- [2] L. Yi, V. G. Kim, D. Ceylan, I. Shen, M. Yan, H. Su, C. Lu, Q. Huang, A. Sheffer, and L. Guibas, “A scalable active framework for region annotation in 3d shape collections,” *ACM Transactions on Graphics (TOG)*, vol. 35, pp. 1 – 12, 2016.
- [3] R. Q. Charles, H. Su, M. Kaichun, and L. J. Guibas, “Pointnet: Deep learning on point sets for 3d classification and segmentation,” in *2017 IEEE Conference on Computer Vision and Pattern Recognition (CVPR)*, 2017, pp. 77–85.
- [4] H. Deng, T. Birdal, and S. Ilic, “Ppfnet: Global context aware local features for robust 3d point matching,” in *2018 IEEE/CVF Conference on Computer Vision and Pattern Recognition*, 2018, pp. 195–205.
- [5] A. V. Phan, M. L. Nguyen, Y. L. H. Nguyen, and L. T. Bui, “Dgcn: A convolutional neural network over large-scale labeled graphs,” *Neural Networks*, vol. 108, pp. 533 – 543, 2018. [Online]. Available: <http://www.sciencedirect.com/science/article/pii/S0893608018302636>
- [6] H. Thomas, C. R. Qi, J. Deschaud, B. Marcotegui, F. Goulette, and L. Guibas, “Kpconv: Flexible and deformable convolution for point clouds,” in *2019 IEEE/CVF International Conference on Computer Vision (ICCV)*, 2019, pp. 6410–6419.
- [7] Z. Gojcic, C. Zhou, J. D. Wegner, and A. Wieser, “The perfect match: 3d point cloud matching with smoothed densities,” in *2019 IEEE/CVF Conference on Computer Vision and Pattern Recognition (CVPR)*, 2019, pp. 5540–5549.
- [8] A. E. Johnson and M. Hebert, “Using spin images for efficient object recognition in cluttered 3d scenes,” *IEEE Transactions on Pattern Analysis and Machine Intelligence*, vol. 21, no. 5, pp. 433–449, 1999.
- [9] A. Frome, D. Huber, R. Kolluri, T. Bülow, and J. Malik, “Recognizing objects in range data using regional point descriptors,” vol. 3, 05 2004, pp. 224–237.
- [10] F. Tombari, S. Salti, and L. Di Stefano, “Unique shape context for 3d data description,” 01 2010.
- [11] S. Salti, F. Tombari, and L. Di Stefano, “Shot: Unique signatures of histograms for surface and texture description,” *Computer Vision and Image Understanding*, vol. 125, 08 2014.
- [12] R. Rusu, N. Blodow, Z. Marton, and M. Beetz, “Aligning point cloud views using persistent feature histograms,” 09 2008, pp. 3384–3391.
- [13] R. B. Rusu, N. Blodow, and M. Beetz, “Fast point feature histograms (fpfh) for 3d registration,” in *2009 IEEE International Conference on Robotics and Automation*, 2009, pp. 3212–3217.
- [14] D. Maturana and S. Scherer, “Voxnet: A 3d convolutional neural network for real-time object recognition,” in *2015 IEEE/RSJ International Conference on Robotics and Automation*, 2015, pp. 1280–1287.

Conv method	R-MSE	R-RMSE	R-MAE	T-MSE	T-RMSE	T-MAE
channel-wise	0.040420	0.201046	0.105576	0.000000	0.000149	0.000094
circular conv	0.017159	0.130991	0.064475	0.000000	0.000048	0.000027
Kernel	R-MSE	R-RMSE	R-MAE	T-MSE	T-RMSE	T-MAE
19	0.017159	0.130991	0.064475	0.000000	0.000048	0.000027
7	0.044989	0.212106	0.123594	0.000000	0.000062	0.000041
KNN	R-MSE	R-RMSE	R-MAE	T-MSE	T-RMSE	T-MAE
10	0.017159	0.130991	0.064475	0.000000	0.000048	0.000027
2	0.014517	0.120486	0.065029	0.000000	0.000037	0.000025
Global information	R-MSE	R-RMSE	R-MAE	T-MSE	T-RMSE	T-MAE
X	0.017159	0.130991	0.064475	0.000000	0.000048	0.000027
O	0.012490	0.111758	0.052873	0.000000	0.000053	0.000027

TABLE IV: Parameter and ablation study

Conference on Intelligent Robots and Systems (IROS), 2015, pp. 922–928.

[15] C. Ruizhongtai Qi, H. Su, M. NieBner, A. Dai, M. Yan, and L. Guibas, “Volumetric and multi-view cnns for object classification on 3d data,” 06 2016, pp. 5648–5656.

[16] G. Riegler, A. O. Ulusoy, and A. Geiger, “Octnet: Learning deep 3d representations at high resolutions,” in *2017 IEEE Conference on Computer Vision and Pattern Recognition (CVPR)*, 2017, pp. 6620–6629.

[17] B. Graham, “Spatially-sparse convolutional neural networks,” 2014.

[18] C. Choy, J. Gwak, and S. Savarese, “4d spatio-temporal convnets: Minkowski convolutional neural networks,” 06 2019, pp. 3070–3079.

[19] C. Choy, J. Park, and V. Koltun, “Fully convolutional geometric features,” in *2019 IEEE/CVF International Conference on Computer Vision (ICCV)*, 2019, pp. 8957–8965.

[20] C. R. Qi, L. Yi, H. Su, and L. J. Guibas, “Pointnet++: Deep hierarchical feature learning on point sets in a metric space,” in *Advances in Neural Information Processing Systems 30: Annual Conference on Neural Information Processing Systems 2017, 4-9 December 2017, Long Beach, CA, USA, I. Guyon, U. von Luxburg, S. Bengio, H. M. Wallach, R. Fergus, S. V. N. Vishwanathan, and R. Garnett, Eds.*, 2017, pp. 5099–5108. [Online]. Available: <http://papers.nips.cc/paper/7095-pointnet-deep-hierarchical-feature-learning-on-point-sets-in-a-metric-space.pdf>

[21] H. Deng, T. Birdal, and S. Ilic, “Ppf-foldnet: Unsupervised learning of rotation invariant 3d local descriptors,” in *ECCV*, 2018.

[22] Y. Wang and J. Solomon, “Deep closest point: Learning representations for point cloud registration,” 10 2019, pp. 3522–3531.

[23] J. Yang, H. Li, D. Campbell, and Y. Jia, “Go-icp: A globally optimal solution to 3d icp point-set registration,” *IEEE Transactions on Pattern Analysis and Machine Intelligence*, vol. 38, no. 11, pp. 2241–2254, 2016.

[24] Q.-Y. Zhou, J. Park, and V. Koltun, *Fast Global Registration*, 2016, pp. 766–782. [Online]. Available: <https://app.dimensions.ai/details/publication/pub.1034541096>

[25] Y. Aoki, H. Goforth, R. A. Srivatsan, and S. Lucey, “Pointnetlk: Robust efficient point cloud registration using pointnet,” in *2019 IEEE/CVF Conference on Computer Vision and Pattern Recognition (CVPR)*, 2019, pp. 7156–7165.

[26] A. Brock, T. Lim, J. Ritchie, and N. Weston, “Generative and discriminative voxel modeling with convolutional neural networks,” Dec. 2016, pp. 1–9, workshop contribution; Neural Information Processing Conference : 3D Deep Learning, NIPS ; Conference date: 05-12-2016 Through 10-12-2016. [Online]. Available: <https://nips.cc/Conferences/2016>

[27] M. Simonovsky and N. Komodakis, “Dynamic edge-conditioned filters in convolutional neural networks on graphs,” in *2017 IEEE Conference on Computer Vision and Pattern Recognition (CVPR)*, 2017, pp. 29–38.

[28] R. Klokov and V. Lempitsky, “Escape from cells: Deep kd-networks for the recognition of 3d point cloud models,” in *2017 IEEE International Conference on Computer Vision (ICCV)*, 2017, pp. 863–872.

[29] Y. Li, R. Bu, M. Sun, W. Wu, X. Di, and B. Chen, “Pointcnn: Convolution on x-transformed points,” in *NeurIPS*, 2018.

[30] M. Atzmon, H. Maron, and Y. Lipman, “Point convolutional neural networks by extension operators,” *ACM Trans. Graph.*, vol. 37, no. 4, Jul. 2018. [Online]. Available: <https://doi.org/10.1145/3197517.3201301>

[31] H. Su, V. Jampani, D. Sun, S. Maji, E. Kalogerakis, M.-H. Yang, and J. Kautz, “Splatnet: Sparse lattice networks for point cloud processing,” 06 2018, pp. 2530–2539.

[32] W. Wang, R. Yu, Q. Huang, and U. Neumann, “Sgpn: Similarity group proposal network for 3d point cloud instance segmentation,” in *2018 IEEE/CVF Conference on Computer Vision and Pattern Recognition*, 2018, pp. 2569–2578.

[33] B. Graham, M. Engelcke, and L. v. d. Maaten, “3d semantic segmentation with submanifold sparse convolutional networks,” in *2018 IEEE/CVF Conference on Computer Vision and Pattern Recognition*, 2018, pp. 9224–9232.

[34] L. Yi, H. Su, X. Guo, and L. Guibas, “Syncspecnn: Synchronized spectral cnn for 3d shape segmentation,” in *2017 IEEE Conference on Computer Vision and Pattern Recognition (CVPR)*, 2017, pp. 6584–6592.

[35] Q. Huang, W. Wang, and U. Neumann, “Recurrent slice networks for 3d segmentation of point clouds,” in *2018 IEEE/CVF Conference on Computer Vision and Pattern Recognition*, 2018, pp. 2626–2635.

[36] C. Wang, B. Samari, and K. Siddiqi, *Local Spectral Graph Convolution for Point Set Feature Learning: 15th European Conference, Munich, Germany, September 8-14, 2018, Proceedings, Part IV*, 09 2018, pp. 56–71.

[37] J. Li, B. M. Chen, and G. H. Lee, “So-net: Self-organizing network for point cloud analysis,” in *2018 IEEE/CVF Conference on Computer Vision and Pattern Recognition*, 2018, pp. 9397–9406.

[38] Y. Xu, T. Fan, M. Xu, L. Zeng, and Y. Qiao, “Spidercnn: Deep learning on point sets with parameterized convolutional filters,” 03 2018.

[39] P. Hermosilla, T. Ritschel, P.-P. Vazquez Alcocer, A. Vinacua, and T. Ropinski, “Monte carlo convolution for learning on non-uniformly sampled point clouds,” vol. 37, 12 2018, pp. 1–12.

[40] F. Groh, P. Wieschollek, and H. Lensch, *Flex-Convolution: Million-Scale Point-Cloud Learning Beyond Grid-Worlds*, 05 2019, pp. 105–122.